ANL/MSD/PP--82718

Epitaxial growth of bcc transition metal films and superlattices onto MgO (111), (011), and (001) substrates*

J.E. Mattson, Eric E. Fullerton, C.H. Sowers, and S.D. Bader

Materials Science Division
Argonne National Laboratory, Argonne, IL 60439

jmc

*Work supported by the U.S. Department of Energy, Basic Energy Sciences-Materials Sciences, under contract #W-31-109-ENG-38.

DISCLAIMER

Portions of this document may be illegible in electronic image products. Images are produced from the best available original document.

Epitaxial growth of bcc transition metal films and superlattices onto MgO (111), (011) and (001) substrates

J. E. Mattson, Eric E. Fullerton, C. H. Sowers,
and S.D. Bader

Materials Science Division, Argonne National Laboratory, Argonne, Illinois 60439

We demonstrate epitaxial growth of the bcc transition metals Nb, Mo, Fe, and Cr via sputtering onto single crystal MgO substrates. The epitaxial growth orientations are (011), (112) and (001) when grown onto MgO (111), (011) and (001), respectively. Further we demonstrate that under appropriate growth conditions, superlattices of these materials (*e.g.* Fe/Cr, Fe/V and Mo/V) can be grown with the same epitaxial order as the films.

PACS# 81.15Cd, 78.70.Ck, 68.55.Gi

I. Introduction

The growth of single-crystal epitaxial metallic thin films and superlattices is of current interest.[1] This interest arises in part because epitaxial films and superlattices elucidate the role of crystal orientation and structure on physical properties such as magnetic anisotropies,[2-4] interlayer coupling,[5-7] elastic response of interfaces,[8] and the superconductivity of layered materials.[9] In most of the work in the literature on epitaxial films, molecular beam epitaxy (MBE) techniques were used. In contrast most studies where films are produced via sputtering, only textured growth is observed with little or no in-plane order. In spite of this association of sputtering and textured films, there has been considerable success in growing epitaxial films and superlattices using sputtering techniques. In particular, high quality epitaxial films of Fe(211),[10] Co/Pt,[11] Pt,[12] Co,[13] Fe/Cr,[7] NbN,[14] NiO/CoO,[15] Nb[16] and YBaCuO[17] have all been successfully grown by sputtering. Referrence 12 showed that three orientations of Pt could be deposited on different orientations of MgO.

The present work is motivated by the studies of the magnetic coupling across non-magnetic spacer-layers. In particular it has been suggested theoretically that the period of oscillation of the coupling should vary depending on the crystalline orientation of the spacer-layer.[5,18,19] The purpose of this work is to establish that one can simultaneously grow three different orientations of the transition metals Nb, Mo, Cr and Fe by the proper choice of substrate and deposition temperature, and further that this epitaxial orientation can be maintained in superlattices (e.g. Fe/Cr, Fe/V, etc.).

The films and superlattices prepared for this study were all made using a Microscience Researcher 1000, equipped with dc magnetron sputtering guns. A computer controlled stepper motor rotated the sample over the targets, allowing the production of the superlattices. The base pressure before deposition was 1×10^{-7} Torr. The Argon pressure during deposition was kept at 3 mTorr and the purity of the Argon gas was 99.999%. The purity of the targets was Nb (99.98%), Mo (99.9%), Cr(99.9%) and Fe(99.7%). The target to substrate distance used was 9cm. The substrate temperature was 600°C for the thick films and for the seed layers in the superlattices which were ~3000Å and ~100Å thick respectively. The Fe/Cr and Fe/V superlattice structures were grown on the seed layers at 200°C and the V/Mo superlattices were grown at 800°C. The single-crystal MgO substrates used were obtained from Electronic Space Products and were epitaxially polished on one side. Films were prepared by placing one of each of the three different orientations of MgO in the sample holder side-by-side so that the three different orientations were prepared simultaneously.

The epitaxy of the films was determined using x-ray diffraction (XRD) techniques using $Cu_{K\alpha}$ radiation. Standard θ-2θ, and rocking curve (in θ) scans were performed to determine the growth direction and mosaic spread in the growth direction of the films. The in-plane epitaxial relationship between the film and substrate, as well as possible twinning in the film, were determined using a rotating anode source equipped with a four-circle goiniometer. The scattering geometry used is one in which a component of the scattering vector is in the plane of the film, and then scanning about the angle ϕ, (in the plane perpendicular to the growth direction).

This paper is organized as follows: Sections II and III discuss out-of-plane and in-plane XRD studies of the thick films on MgO (001), (011) and (111), respectively. Section IV discusses the results of growing epitaxial superlattices of Fe/Cr, Fe/V and V/Mo. We summarize the results in Section V.

II. Results

A. Out-Of-Plane XRD Results

The results of the XRD measurements with the scattering vector normal to the plane of the film are shown in Fig. 1 for films grown on MgO(001), (011) and (111) substrates. From this it is quite clear that the bcc metals Nb, Mo, Cr and Fe grow with a preferred

(001), (112) and (011) orientation, respectively and the contribution of any secondary orientations are suppressed by a factor of a 100 or more. Further information about the film can be determined from the position of the Bragg reflections, its full-width at half-maximum (FWHM) and the mosaic spread (determined from the FWHM of the rocking curve). The position of the Bragg reflections in each film indicates that there is no measurable strain, as expected for such thick films. The FWHM of the Bragg peaks allow us to determine the length scale (in the growth direction) over which the film is structurally coherent. The results are shown in Table I. These numbers are only upper bounds on the FWHM since the angular resolution of the diffractometer is only ~0.15°. Thus, the determination of the FWHM in many of the films is limited by the instrumental resolution. The films grown on MgO(001) substrates all have a FWHM of ~0.15°, placing a lower limit on the coherence length of ~600Å, indicative of high-quality films. The films grown on MgO(011) have similar structural coherence and quality. However, the Mo and Nb films show a somewhat deteriorated structural quality as indicated by the slight increase in the FWHM of the Bragg peak. The films grown on MgO(111) show only slightly broader peaks with FWHM ≈ 0.2 - 0.27°, which may result from the miscut of the substrate, as discussed in the next section.

The mosaic spread of the Bragg peaks for the films grown on MgO(001) and (111) are all nearly 0.5°, indicating that the films are aligned to a very high degree. For the MgO(011) films this trend is mirrored in the behavior of the mosaic spread of the Bragg peaks for Fe and Cr but increase slightly for Mo and significantly for Nb (2.4°). Nevertheless, all the films show a high degree of orientation. Despite the large lattice mismatch between MgO and the Mo and Nb films, and the presence of a large asymmetric mismatch between the (112) oriented films and the MgO (011) substrate, all oe the films grow with excellent structural coherence and mosaic spread.

B. In-Plane XRD Results

The quality of the out-of-plane data suggest that the films are epitaxially oriented to the substrates. To explore this, asymmetric diffraction scans were performed on the Mo films. To determine the in-plane orientation, the sample was first aligned optically to within ≈ 1° of the surface normal, the diffractometer was then aligned to the MgO normal direction and to a reflection away from the surface normal [*e.g.* the MgO (022) reflection for the MgO (001) substrate]. In this way large (>3°) miscuts could be determined. The films were then similarly aligned to the Mo normal direction and to an off-normal reflection, such as the Mo (011) for the Mo(001) films. This determined both the direction of the film normal and the relative in-plane orientation of the Mo with respect to the substrate. This was followed by performing a ϕ scan wherein the sample is rotated about the normal of the Mo film while in the scattering condition for the off-normal reflection. This allows verification of the symmetry and provides an estimate of the in-plane mosaic spread. This procedure also allows us to determine if twinning is present. One cautionary note is that under the above procedure we can probe twinned grains only if the growth direction of the twinned region is not more than ~1° misaligned with respect to the growth direction of the untwinned region.

(i) Mo(001) on MgO(002)

The in-plane epitaxial order of the Mo(001) films on MgO(002) were explored by first aligning to the MgO(002) and (022) reflections and then aligning to the Mo (002) and (022) directions. This showed the film and substrate to be aligned in the growth direction to better than ±0.2°. The result of the ϕ scan while in the scattering conditions for the Mo(011) plane is shown in Fig. 2a. From this data the epitaxial relationship shown in Fig. 2b is derived. Similar epitaxial relationships have been observed for MBE grown Fe and Cr films, and epitaxial Fe/Cr superlattices.[20] Thus for these bcc metal films the in-plane

Mo$[11\bar{1}]$//MgO$[02\bar{2}]$. The ϕ scan reveals that there is a weak signal from a twinned grain. The surprising feature is that one would expect three possible twinning orientations each rotated by 120° from the other. However, in these films only a weak second twin orientation is observed. This may result from the 7° miscut of the MgO stabilizing a particular twin orientation, or to the possibility of the twinned grains being misaligned in the growth direction by more than ~1° and missed by the ϕ scan.

C bcc/bcc Epitaxial Superlattices

Both Fe and Cr grow epitaxially on MgO(001), MgO(011) and MgO(111), as shown already. Therefore, it should not be surprising that since Fe and Cr are nearly latticed matched, that they should grow well as a superlattice. The data for the Fe/Cr superlattices grown on MgO(001) and MgO(011) have been discussed elsewhere.[7] To summarize those results, the same epitaxial relationships exist for the Fe/Cr superlattices as exist for the Fe and Cr films. More specifically, for the (001) oriented films the Fe and Cr[100] directions are parallel to each other and rotated by 45° with respect to the MgO[100]. For the (112) oriented films the in-plane Fe(and Cr) $[1\bar{1}0]$ directions are parallel to each other and parallel to the MgO[100] directions.

Both Fe/V and Mo/V have a modest mismatch of ≈5%. However Fe and V should grow quite well as a superlattice under the same growth conditions as the Fe/Cr superlattices. A 100-Å seed layer of Cr on MgO was used to stabilize the film growth with the same growth orientation as the Fe films on MgO. This is shown in the high-angle XRD in Fig 5 where the scattering vector is normal to the plane of the film. Figure 5a, b and c show the Fe/V superlattices grown on MgO(100), (110) and (111), respectively. The coherence lengths seen in these films are quite large (≈400Å) for all of the films. The high-angle XRD spectra all indicate that Fe/V grows as high quality superlattices. However, low-angle XRD show that these superlattices have significantly increased layer-roughness, as indicated by a deteriorated low-angle spectra.

The Mo/V system did not grow well as a superlattice at the growth temperature of 200°C, as has been seen by others who found the optimum growth temperature of the (100) orientation to be 800°C[21]. The high-angle XRD spectra are shown in Fig. 7 for Mo/V films grown at 800°C on a 100-Å Mo base-layer also grown at 800°C. It is clear from these spectra that though the growth orientation of the films is still (001), (011) and (112) for films grown on MgO(001), (111) and (011), respectively, that only the (001) oriented films show high-quality (small FWHM and mosaic spread) growth. Further, as seen in other studies on Mo/V superlattices,[21] growing the (001) oriented films at 800°C improves the quality of the films. However, the (011) and (112) oriented films do not show similar improvements at higher growth temperature. Low-angle XRD indicates that the (001) oriented films are well layered, whereas the (011) and (112) oriented films have significant layer roughness as indicated by a deteriorated spectra. Nevertheless, highly oriented Mo/V superlattices with three different orientations can be grown simultaneously.

III Summary

We have shown that the epitaxial growth of the transition metals Nb, Mo, Cr and Fe on the MgO(001), (011) and (111) surfaces result in epitaxial (001), (112) and (011) oriented films. This is achieved even for the growth of Nb, in spite of the relatively large lattices mismatch between MgO and Nb of 10.9%. This same epitaxial growth can be maintained in the growth of superlattices such as Fe/Cr, Fe/V and Mo/V. However, for the superlattices the thermodynamics of the growth for the different orientations may require slightly different growth conditions for each of the different crystalline orientations for optimal growth to be achieved. Further improvements in film growth or the lowering of the optimum substrate temperature may also occur for different initial seed layers.[12] Regardless, high quality epitaxial films and superlattices of the transition metals Fe, Cr, V, Mo, and Nb can be simultaneously grown via sputtering on MgO(100), (110) and (111) substrates.

The ability to grow high-quality films and superlattices permits the study of effects of crystallographic orientation and structural quality on the magnetic, superconducting and elastic properties. For example, sputtered epitaxial Fe/Cr superlattices have shown unambiguously that the period, phase and strength of the antiferromagnetic coupling along the Cr (001) and (112) directions are identical.[7] Further, the combination of the uniaxial magnetic anisotropy and strong antiferromagnetic coupling have permitted the first observation of the surface spin-flop transition.[22] These, and other effects await the study of high-quality epitaxial films, such as can now be produced by sputtering.

IX ACKNOWLEDGMENTS

The authors would like to thank Hoydoo You for the use of his rotating anode four-circle diffractometer. This work was supported by the U.S. Department of Energy, BES-Materials Sciences, under contract W-31-109-ENG-38.

FIGURE CAPTIONS:

1 θ–2θ XRD scans, with the scattering vector normal to the plane of the film, (from top to bottom) of Nb, Mo, Cr and Fe. The left column is for samples made on MgO(001), the center column is for samples made on MgO(110) and the right column is for samples made on MgO(111).

2 a) ϕ scan of Mo (022) reflection for Mo(001) oriented films. The angle ϕ, is measured relative to the MgO[020] direction. b) The epitaxial relationship between MgO and Mo determined from this scan.

3 a) ϕ scan of Mo (220) reflection for Mo(112) oriented films. The angle ϕ, is measured relative to the MgO[$2\bar{1}1$] direction. b) The epitaxial relationship between MgO and Mo determined from this scan.

4 a) ϕ scan of Mo (020) reflection for Mo(011) oriented films. The angle ϕ, is measured relative to the MgO[$11\bar{2}$] direction. b) The epitaxial relationship between MgO and Mo determined from this scan.

5 High-angle XRD spectra for a $[Fe(15Å)/V(28Å)]_{20}$ superlattice grown on: a) MgO(001); b) MgO(110); and c) MgO(111) substrates.

6 High-angle XRD spectra for a $[Mo(10Å)/V(10Å)]_{60}$ superlattice grown on: a) MgO 001); b) MgO(110); and c) MgO(111) substrates.

Table I The measured out-of-plane XRD parameters full width at half maximum (FWHM) of the selected Bragg peak, and the mosaic spread of this peak, for the epitaxial bcc films grown on three different orientations of MgO at 600°C.

	MgO (001)		MgO (011)		MgO (111)	
	FWHM (002)	Mosaic (002)	FWHM (112)	Mosaic (112)	FWHM (110)	Mosaic (110)
Nb	0.17	0.32	0.31	2.4	0.20	0.43
Mo	0.15	0.45	0.20	0.66	0.19	0.35
Cr	0.13	0.50	0.13	0.50	0.27	0.60
Fe	0.13	0.33	0.13	0.36	0.22	0.50

REFERENCES

1. L. M. Falicov, Daniel T. Pierce, S. D. Bader, R. Gronsky, Kristl B. Hathaway, Herbert J. Hopster, David N. Lambeth, S. S. P. Parkin, Gary Prinz, Myron Salamon, Ivan K. Schuller and R. H. Victora, *J. Matter. Res.* **5**, 1299 (1990).
2. Brad N. Engel, Craig D. England, Robert A. Van Leeuwen, Michael H. Wiedmann and Charles M. Falco, *J. Appl. Phys.* **70**, 5873 (1991).
3. P. Bruno and J.-P. Renard, *Applied Physics A* **49**, 499 (1989).
4. H. J. Elmers, T. Furubayashi, M. Albrecht and U. Gradmann, *J. Appl. Phys.* **70**, 5764 (1991).
5. P. Bruno and C. Chappert, *Phys. Rev. B* **46**, 261 (1992).
6. M. T. Johnson, P. J. H. Bloemen, R. Coehoorn, J. J. de Vries, N. W. E. McGee, R. Jungblut, A. Reinders and J. aan de Stegge, *Mater. Res. Soc. Symp.* **313**, 93 (1993).
7. Eric E. Fullerton, M. J. Conover, J. E. Mattson, C. H. Sowers and S. D. Bader, *Phys. Rev. B* **48**, (1993).
8. Ivan K. Schuller, A. Fartash, Eric E. Fullerton and M. Grimsditch, *Mat. Res. Soc. Symp. Proc.* **239**, 499 (1992).
9. Y. Suzuki, D. Lew, A.F. Marshall, M.R. Beasley and T.H. Geballe, *Phys. Rev. B* 48, 10642 (1993).
10. Seiji Yaegashi, Toshiya Kurihara and Hideo Segawa, *J. Appl. Phys.* 74, 4506 (1993).
11. C. H. Lee, R. F. C. Farrow, C. J. Lin, E. E. Marinero and C. J. Chien, *Phys. Rev. B* 42, 11384 (1990).
12. B.M. Lairson, M.R. Visokay, R. Sinclair, S. Hagstrom and B.M. Clemens, *Appl. Phys. Lett.* **61**, 1390 (1992).

13. Ch. Morawe, A. Stierle, N. Metoki, K. Bröhl and H. Zabel, *J. Magn. Magn. Mater.* **102**, 223 (1991).

14. J. Talvacchio and A. I. Braginski, *IEEE Trans. Magn.* Mag-23, 859 (1987).

15. M.J. Carey, F.E. Spada, A.E. Berkowitz, W. Cao and G. Thomas, *J. Mater. Res.* **6**, 2680 (1991).

16. R. E. Somekh, K. H. Huang and W. C. Shih, *Vacuum* **38**, 693 (1988).

17. E. E. Fullerton, J. Guimpel, O. Nakamura and I. K. Schuller, *Phys. Rev. Lett.* **69**, 2859 (1992).

18. M. D. Stiles, *Phys. Rev. B* **48**, 7238-7258 (1993).

19. D. D. Koelling, "Magnetic Mulitlayers with (Nb, Mo and Cr) spacer-layers",*Phys. Rev. B* (1994) in press.

20. P. Etienne, J. Massies, S. Lequien, R. Cabanel and F. Petroff, *J. Cryst. Growth* **111**, 1003 (1991).

21. M. G. Karkut, D. Ariosa, J. -M. Tiscone and Ø. Fischer, *Phys. Rev. B* **32**, 4800 (1985).

22. R. W. Wang, D. L. Mills, E. E. Fullerton, J. E. Mattson and S. D. Bader, *Phys. Rev. Lett.* **72**, 920-923 (1994).

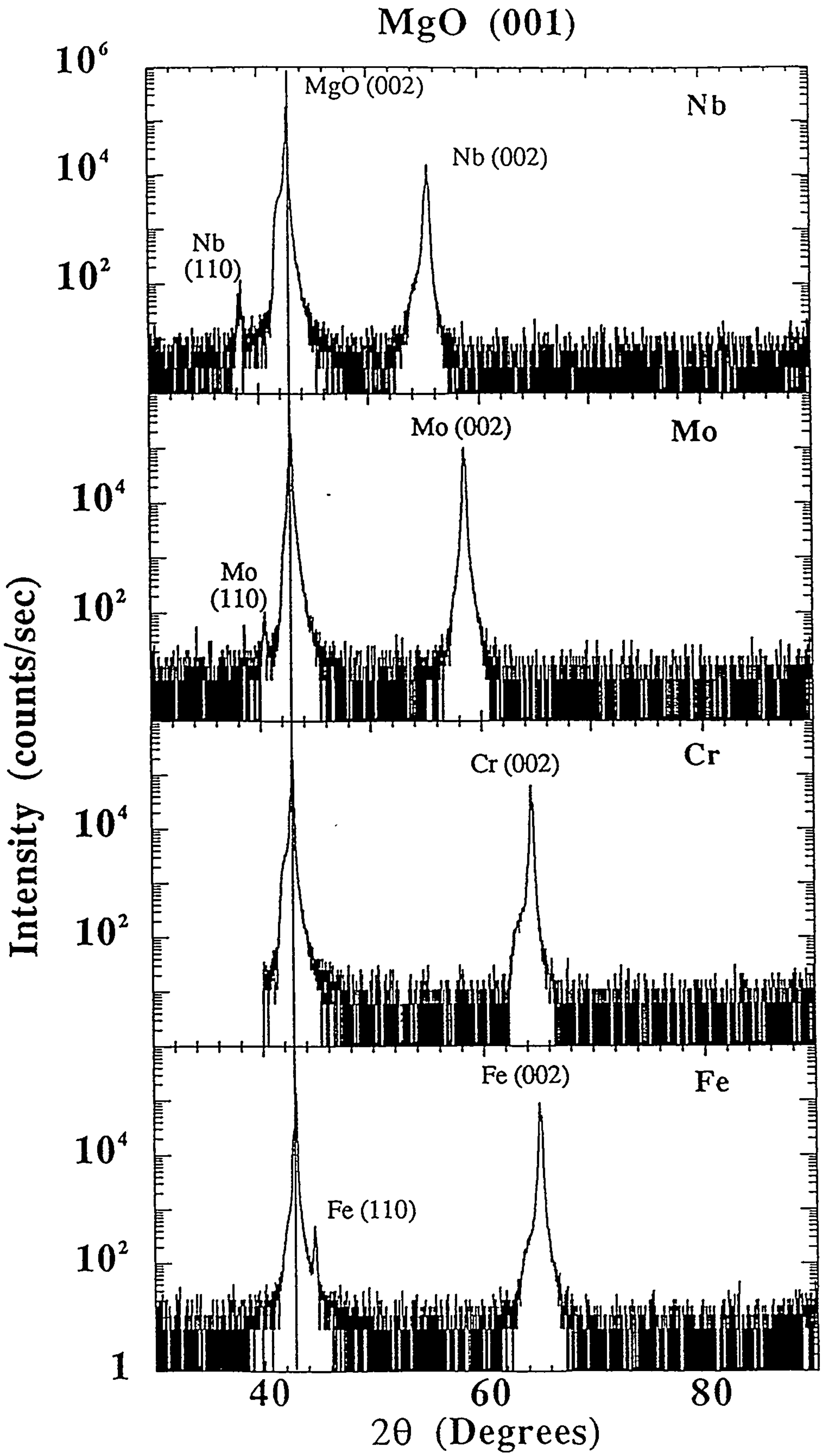

MgO (001)
MgO (002)
Nb
Nb (002)
Nb
(110)
Mo (002)
Mo
Mo
(110)
Cr (002)
Cr
Fe (002)
Fe
Fe (110)
10^6
10^4
10^2
1
Intensity (counts/sec)
40
60
80
2θ (Degrees)

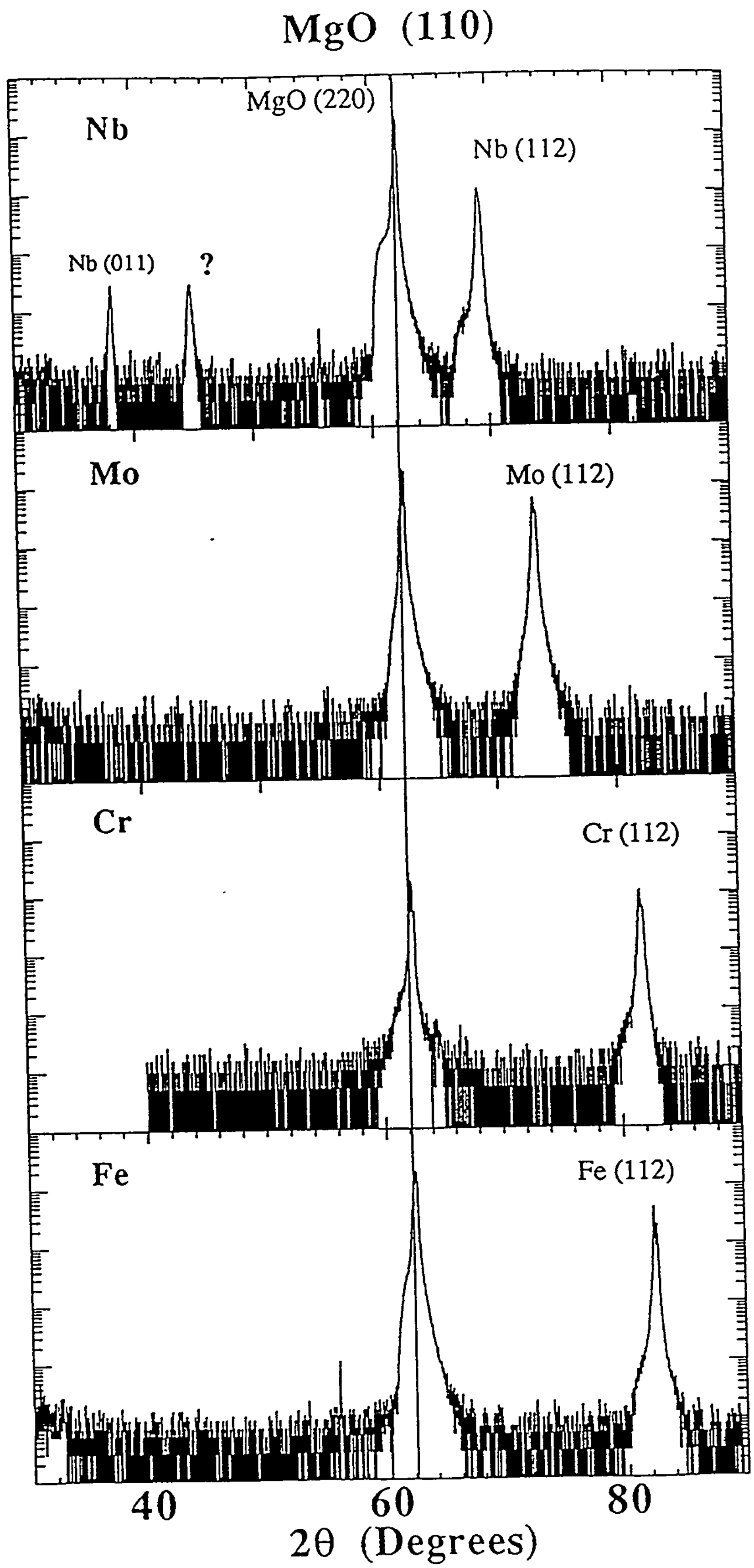
MgO (110)
MgO (220)
Nb
Nb (112)
Nb (011)
?
Mo
Mo (112)
Cr
Cr (112)
Fe
Fe (112)
40
60
80
2θ (Degrees)

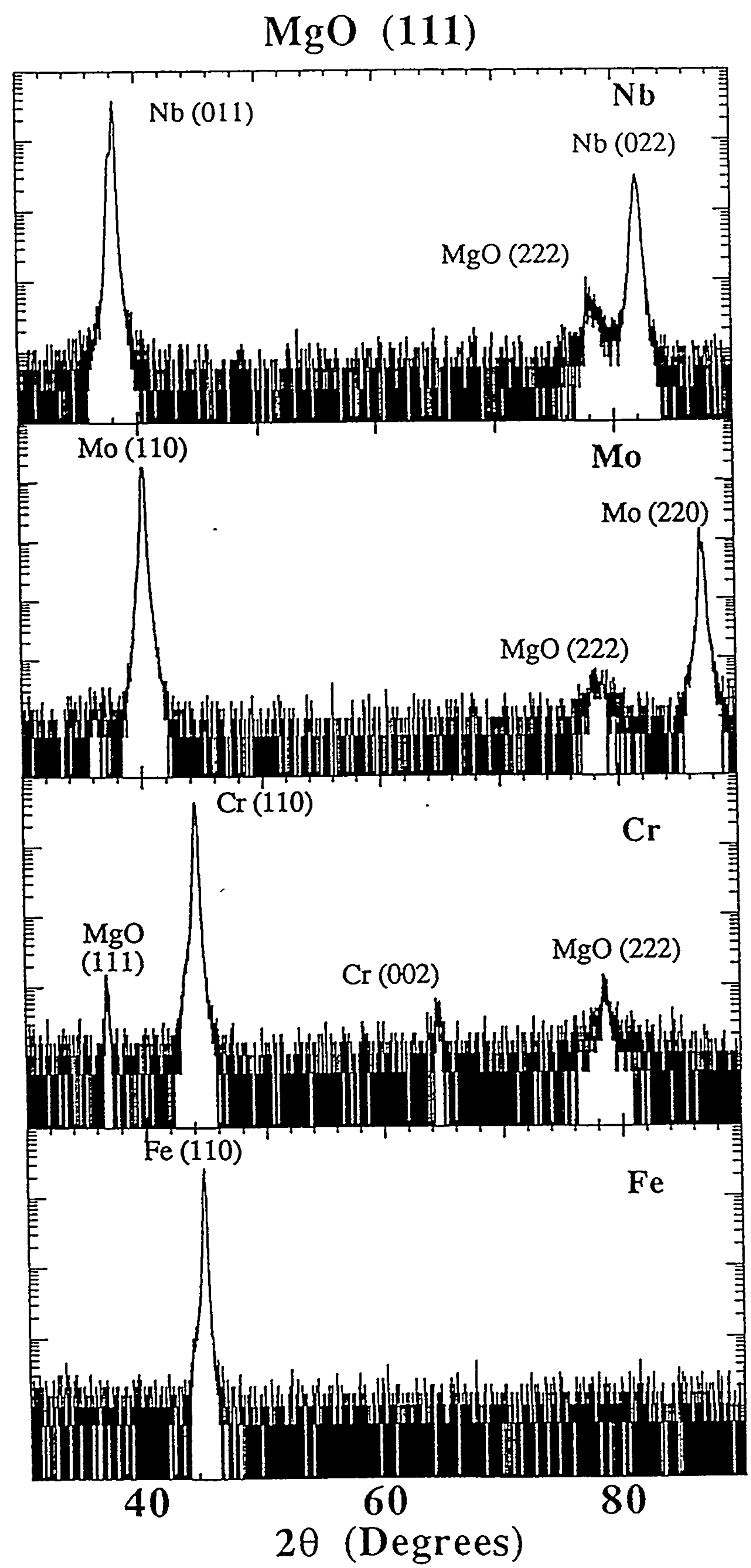

MgO (111)
Nb
Nb (011)
Nb (022)
MgO (222)
Mo
Mo (110)
Mo (220)
MgO (222)
Cr
Cr (110)
MgO
(111)
Cr (002)
MgO (222)
Fe
Fe (110)
40
60
80
2θ (Degrees)

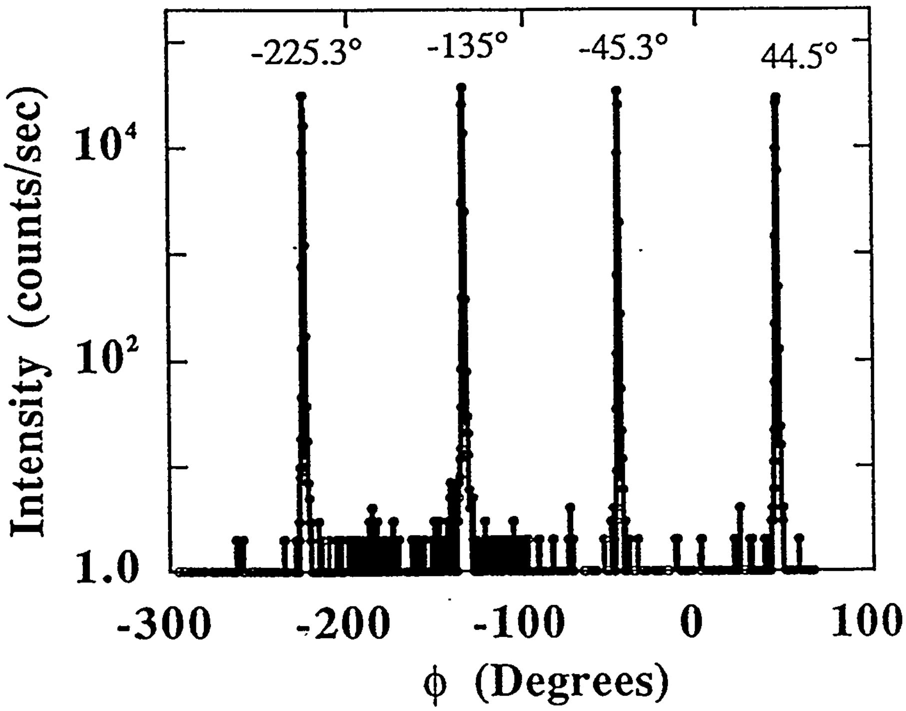
-225.3°
-135°
-45.3°
44.5°
Intensity (counts/sec)
10^4
10^2
1.0
-300
-200
-100
0
100
ϕ (Degrees)

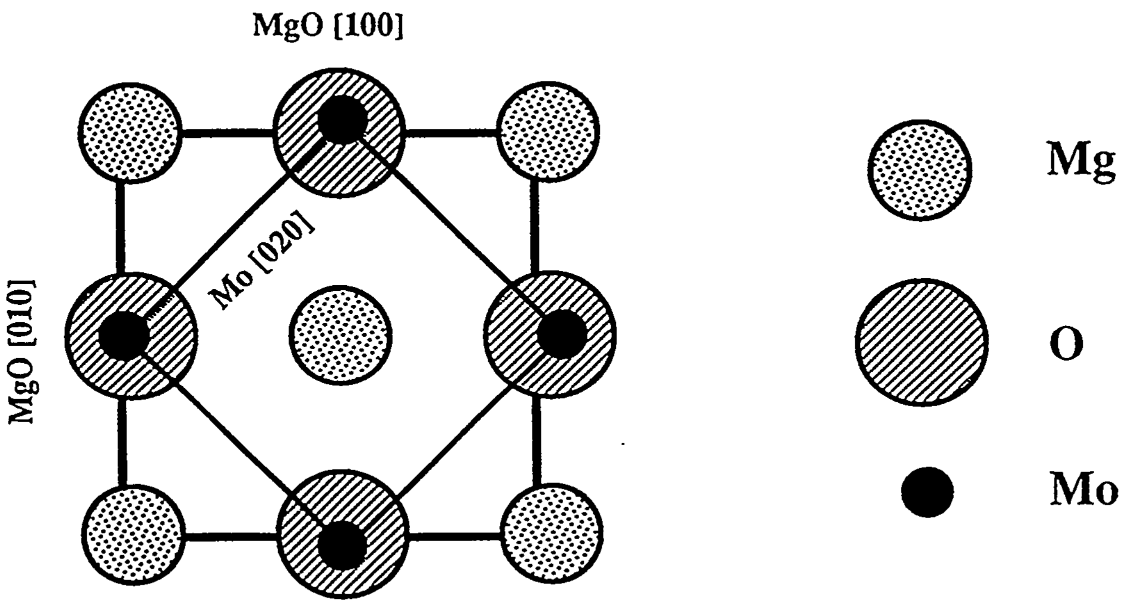

MgO [100]
MgO [010]
Mo [020]
Mg
O
Mo

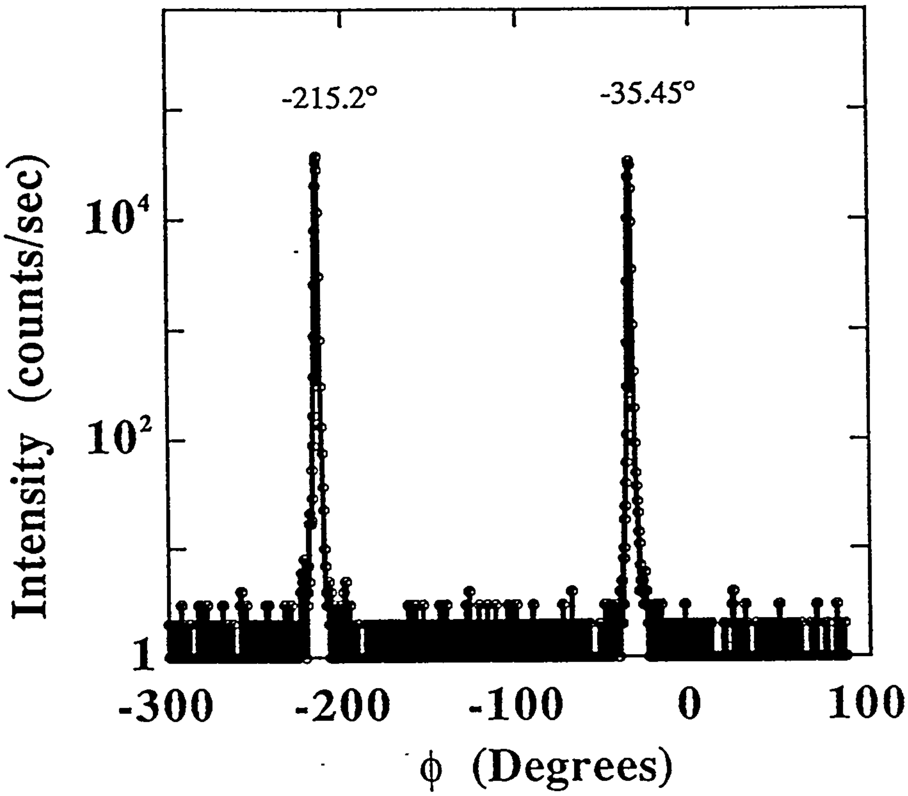

-215.2°
-35.45°
Intensity (counts/sec)
10^4
10^2
1
-300
-200
-100
0
100
φ (Degrees)

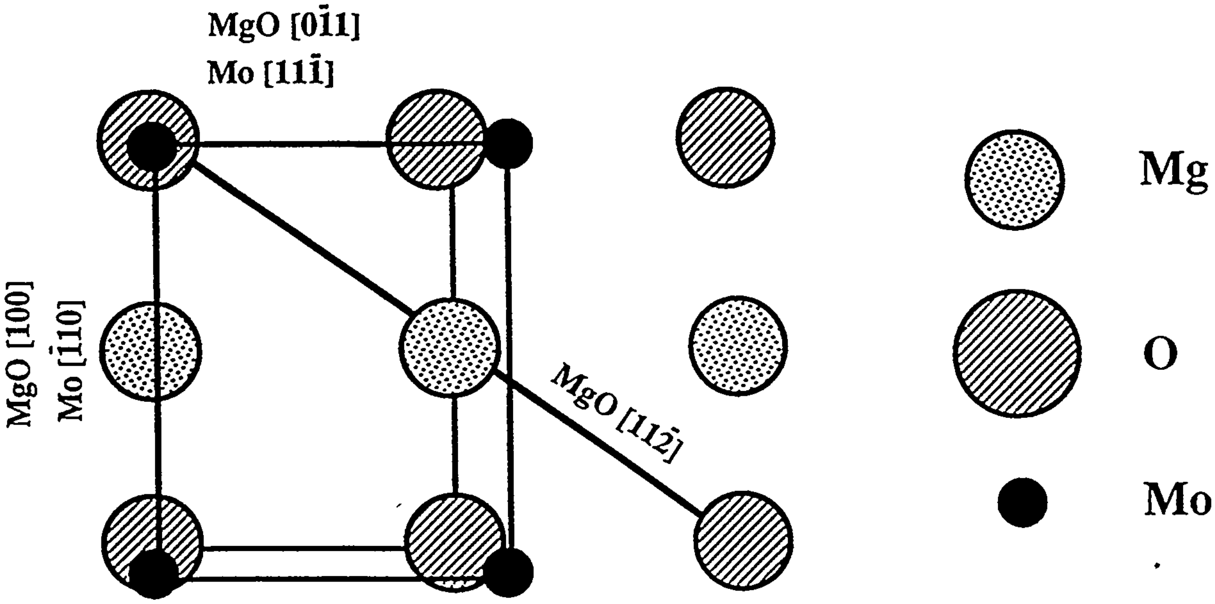
MgO [0$\bar{1}$1]
Mo [11$\bar{1}$]
MgO [100]
Mo [$\bar{1}$10]
MgO [11$\bar{2}$]
Mg
O
Mo

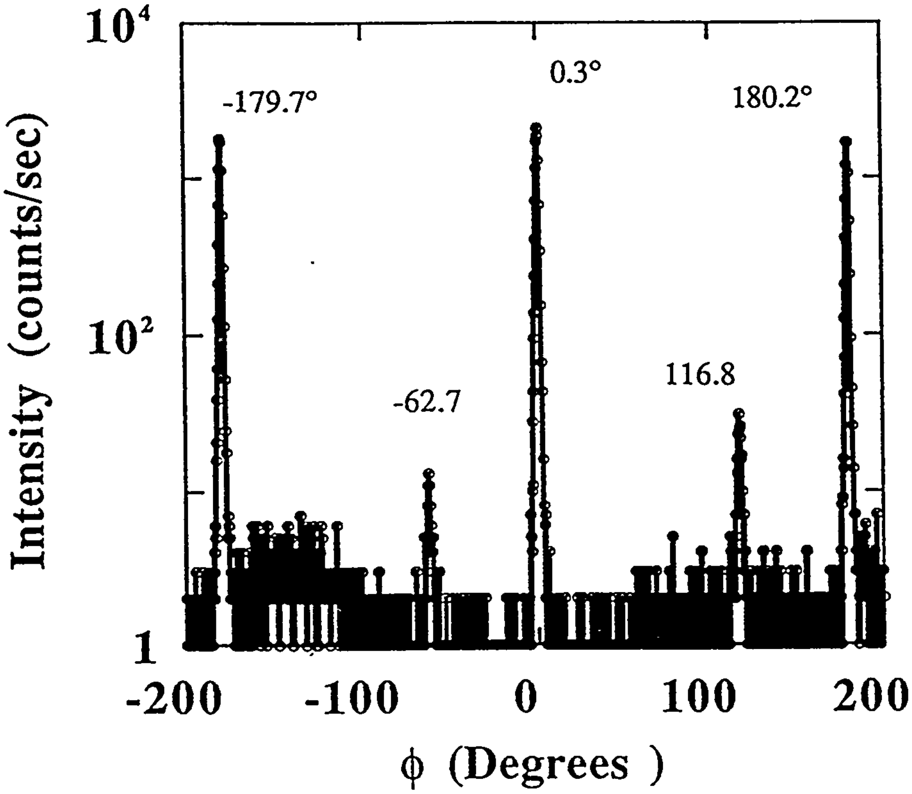

10⁴
10²
1
Intensity (counts/sec)
-179.7°
0.3°
180.2°
-62.7
116.8
-200
-100
0
100
200
ϕ (Degrees)

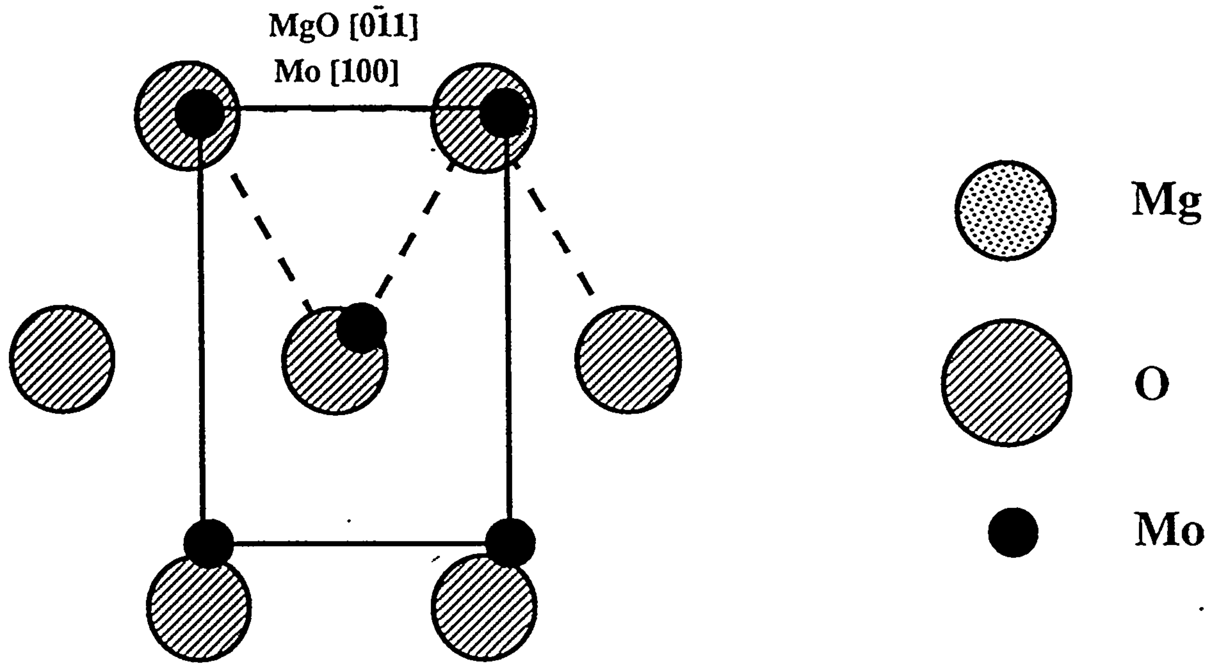
MgO [0$\bar{1}$1]
Mo [100]
Mg
O
Mo

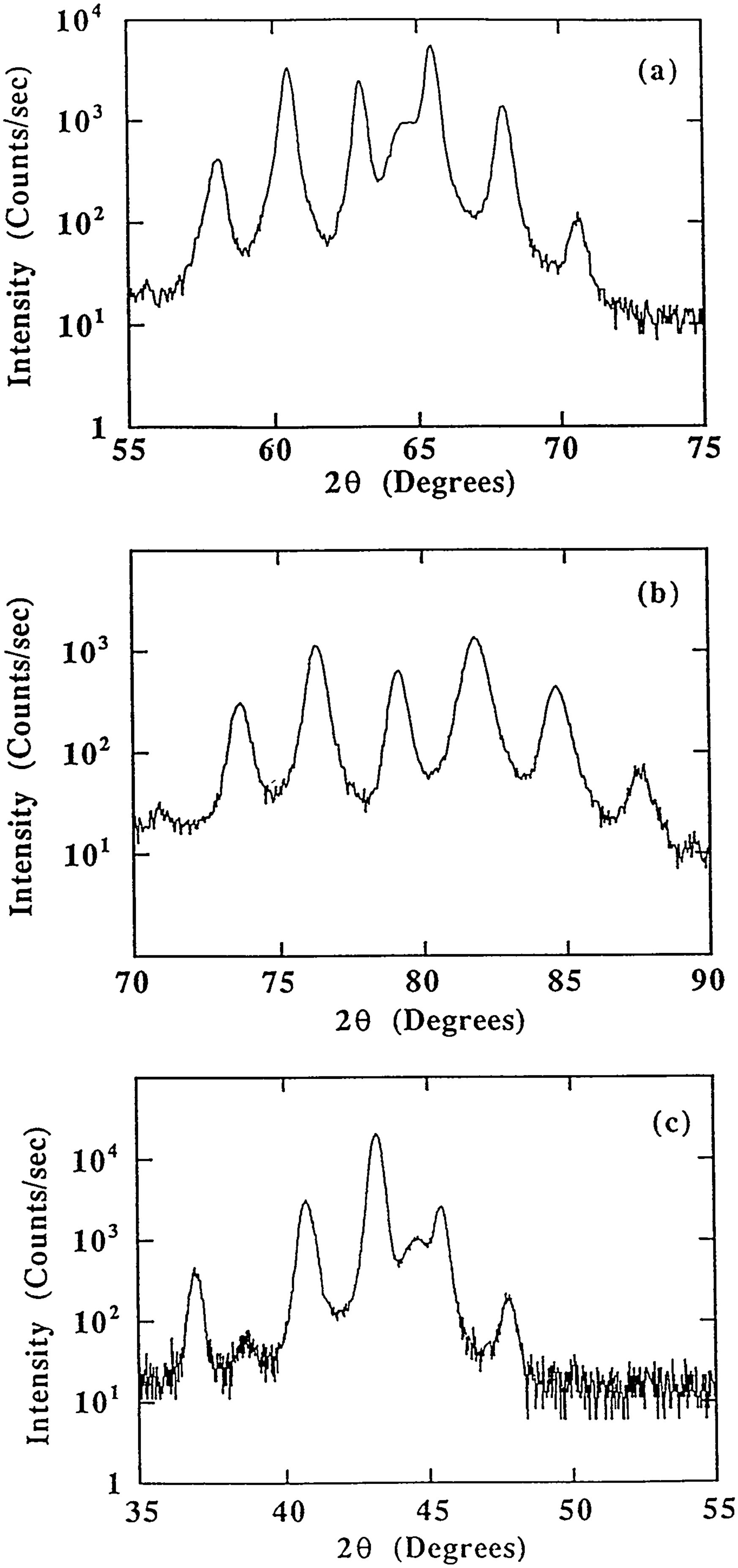
(a)
Intensity (Counts/sec)
2θ (Degrees)
(b)
Intensity (Counts/sec)
2θ (Degrees)
(c)
Intensity (Counts/sec)
2θ (Degrees)

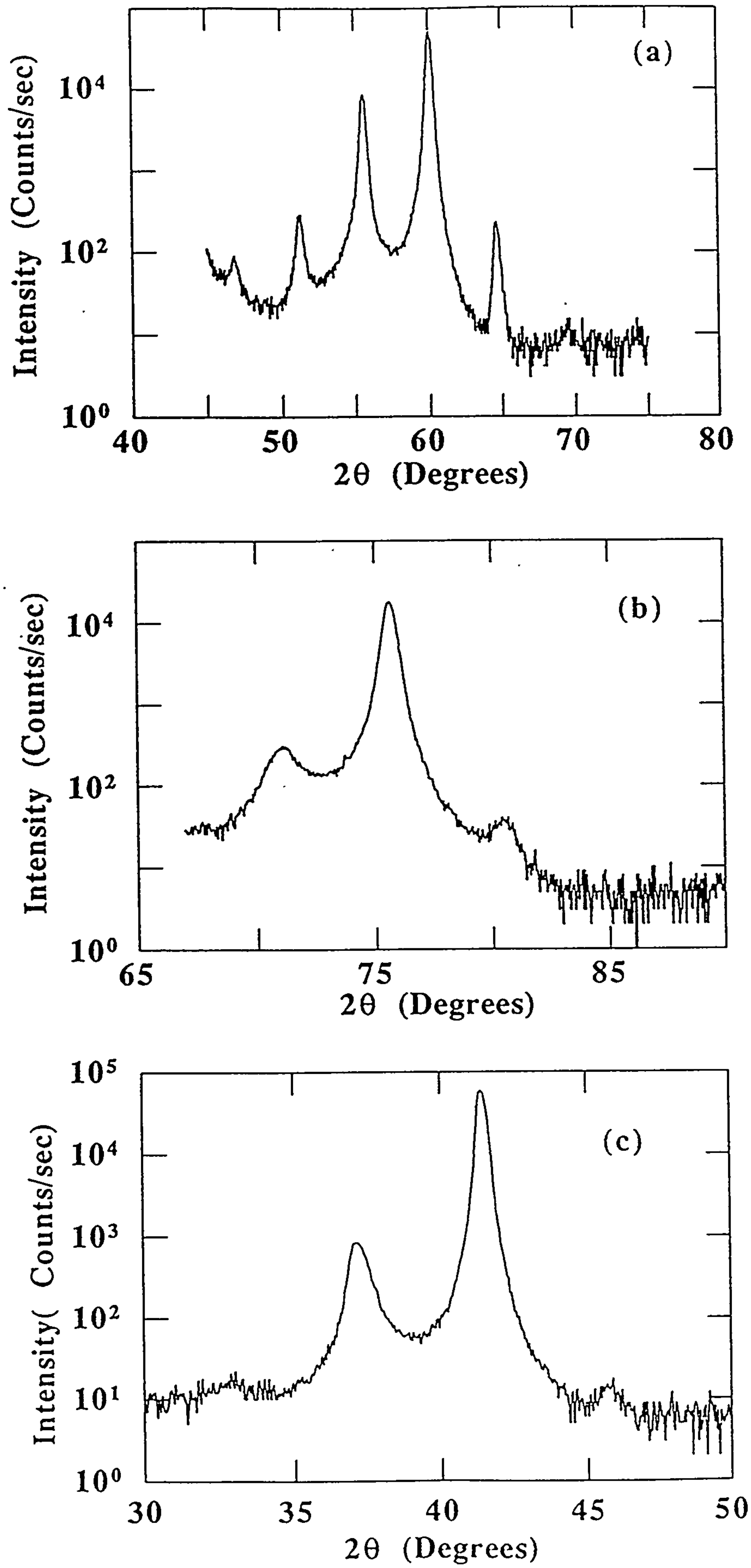

(a)
Intensity (Counts/sec)
10^4
10^2
10^0
40
50
60
70
80
2θ (Degrees)
(b)
Intensity (Counts/sec)
10^4
10^2
10^0
65
75
85
2θ (Degrees)
(c)
Intensity(Counts/sec)
10^5
10^4
10^3
10^2
10^1
10^0
30
35
40
45
50
2θ (Degrees)